Proceeding of the 18th ME-NETT Conference
18-20 October 2004, Khonkean

Stress Intensity Factor Calculation by the Domain Integral Method and Adaptive FEM Remeshing Technique

Kobsak POTJANANAPASIRI, Sutthisak PHONGTHANAPANICH and Pramote DECHAUMPHAI
Department of Mechanical Engineering, Faculty of Engineering,
Chulalongkorn University, 10330, Thailand
Tel: 0-2218-6621 Fax: 0-2218-6621 E-mail: fmepdc@eng.chula.ac.th

Abstract

This paper presents a finite element method for analyzing two-dimensional linear elastic fracture mechanics problems with cracks presented in material bodies. Stress intensity factor is used as the parameter to characterize the severity of the stresses near the crack tip. The domain integral method, for which all relevant quantities are integrated over any arbitrary element area around the crack tip, is utilized as the stress intensity factor solution scheme. The six-node triangular elements are placed around the crack tip. An adaptive remeshing technique is implemented for automatically generating small elements in the regions with high stress gradients to improve solution accuracy. Many benchmark problems are analyzed to demonstrate the efficiency of the numerical solution scheme.

1. Introduction

In linear elastic material behavior, Stress Intensity Factor, SIF, is the most widely used parameter characterizing the intensity of stresses near a crack tip. Many numerical procedures have been developed to estimate the SIF such as stress and displacement matching, contour integration and virtual crack extension [1], etc. One efficient method that has many advantages is the energy domain integral. Originally formulated by Shih, et. al. [2], this approach is remarkably versatile because it can be applied to both quasistatic and dynamic problems with elastic, plastic, or viscoplastic material responses, as well as thermal loading. Moreover, it can numerically be employed to efficiently calculate the other two important elastoplastic crack tip parameters; J and T^*-integral which based respectively on the deformation and incremental theory of plasticity [3].

In this paper, the domain integral method is used to calculate the energy release when a crack grows and convert it to the SIF by relations between stresses and energy. Adaptive remeshing technique and crack tip element in which mid-side nodes near the tip displaced from its nominal positions to quarter points [4] are also implemented to enhance the solution accuracy. Several problems have been analyzed to demonstrate the algorithm.

2. The energy domain integral

For stable crack growth in a two-dimensional body having a line crack along the x_1 axis, the energy release per unit crack advance is,

$$J = \lim_{\Gamma \to 0} \int_{\Gamma} \left(W\delta_{1i} - \sigma_{ij} u_{j,1} \right) n_i dC \tag{1}$$

where W is the stress work density, σ_{ij} and u_i are components of the stress and displacement along the x_i axis, n_i is the unit vector normal to Γ contour and dC is the infinitetesimal arc length as depicted in Fig. 1.

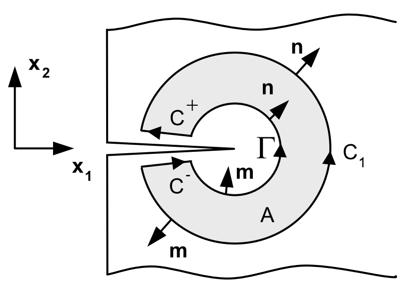

Fig. 1. Closed contour $C = C_1 - \Gamma + C^+ + C^-$ enclosing a simply connected region A

In the absence of thermal strain, body force and crack face traction, Eq. (1) can be rewritten in the form,

$$J = \int_C \left[\sigma_{ij} u_{j1} - W\delta_{1i} \right] m_i q_1 dC \qquad (2)$$

where $C = C_1 + C^+ + C^- - \Gamma$ is the closed curve, q_1 is a sufficiently smooth function in the area enclosed by C which is unity on Γ and zero on C_1, and m_j is the components of outward normal unit vector as shown in Fig. 1. By applying the divergence theorem to (2),

$$J = \int_A \left[\left(\sigma_{ij} u_{j,1} - W\delta_{1\iota} \right) q_1 \right]_{,1} dA \qquad (3)$$

where A is the area enclosed by C. Invoking the equilibrium equation, the domain expression for the energy release rate is,

$$J = \int_A \left[\sigma_{ij} u_{j,1} - W\delta_{1i} \right] q_{1,i} dA \qquad (4)$$

The function q_1 can be interpreted as a unit translation on Γ in the x_1 direction while keeping the material points on C_1 fixed. According to the vanishing of Γ around the tip, this can be viewed as the growing of the crack.

3. Stress intensity factor

In linear elastic material response, the stress intensity factor in opening mode can be computed from the energy release rate by the expression [1],

$$K_I = \sqrt{JE'} \qquad (5)$$

where $E' = E, \dfrac{E}{1-\nu}$ for plane strain and plane stress case respectively, E is the modulus of elasticity, and ν is the Poisson's ratio.

4. Finite element formulation for the domain integral method

For the six-node isoparametric element, the coordinates, displacements, and a smooth function are,

$$x_i = \sum_{K=1}^{6} N_K X_{iK} \qquad (6)$$

$$u_i = \sum_{K=1}^{6} N_K U_{iK} \qquad (7)$$

$$q_1 = \sum_{K=1}^{6} N_K Q_{1K} \qquad (8)$$

where N_K are the shape functions, X_{iK} are the nodal coordinates, U_{iK} are the nodal displacements and Q_{1I} are the nodal values of the smooth function varying between 1 and 0.

Using Eq. (6) and (8) and the chain rule, the spatial gradient of q_1 is,

$$\frac{\partial q_1}{\partial x_j} = \sum_{I=1}^{6} \sum_{k=1}^{2} \frac{\partial N_I}{\partial \eta_k} \frac{\partial \eta_k}{\partial x_j} Q_{1I} \qquad (9)$$

where $\dfrac{\partial \eta_k}{\partial x_j}$ is the inverse Jacobian matrix.

For 2×2 Gaussian integration, the energy release rate expression in Eq. (4) is,

$$J = \sum_{\substack{\text{all} \\ \text{elements} \\ \text{in A}}} \sum_{p=1}^{4} w_p \left\{ \left[\sigma_{ij} \frac{\partial u_j}{\partial x_1} - W\delta_{1i} \right] \frac{\partial q_1}{\partial x_1} \det\left(\frac{\partial x_k}{\partial \eta_k} \right) \right\}_p t \qquad (10)$$

where all quantities are calculated at the 4 Gauss points with w_p as their respective weights and t is the specimen thickness.

5. Crack tip elements and the smooth function

Fig. 2 shows elements and finite element mesh on the domain used in this scheme. In this paper, the six-node rosette elements which the mid-side nodes near a tip located on the one-fourth of their sides from the tip are placed around the crack tip. These element can improve the solution because they have the same $1/\sqrt{r}$ singularity of displacement solutions as the exact solution does at the tip. The other elements out of this rosette are standard six-node isoparametric triangular elements.

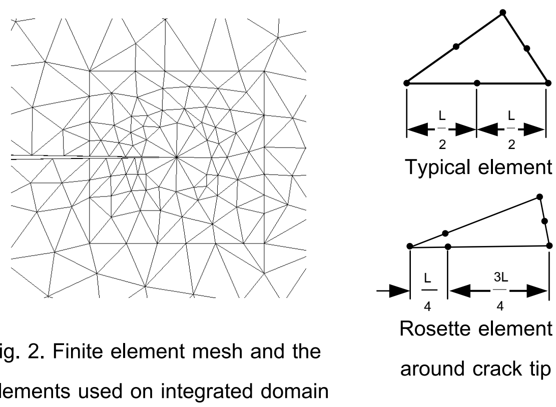

Fig. 2. Finite element mesh and the elements used on integrated domain

According to Shih, et. al. [2], the simple pyramid function as depicted in Fig. 3 is utilized as the smooth function which is unity at the crack tip and varies to zero on the edges of the domain. The base of this pyramid smooth fuction which coincides with the square mesh surrounding the tip is also shown in the figure.

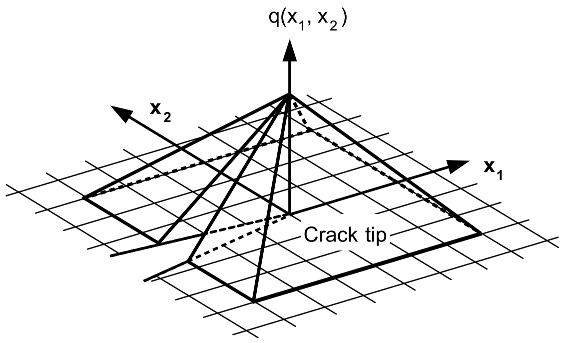

Fig. 3. A smooth function on integrated domain

6. Adaptive remeshing technique

The adaptive remeshing technique generates an entirely new mesh based on the solution obtained from the previous mesh. The technique generates small elements in the regions with large change in the stress gradients to increase the analysis solution accuracy. At the same time, larger elements are generated in the other regions where the stress is nearly uniform to reduce the computational time and the computer memory. The adaptive remeshing procedure thus consists of two main steps: the computation of proper element sizes and the generation of a new mesh for the entire domain.

6.1 Element sizes

To determine proper element sizes at different locations in the domain, the solid mechanics concept for determining the principal stresses from a given state of stresses at a point is employed. Because small elements must be placed in the region where large changes in the stress gradients, such as the von Mises stress σ, occur. Thus the second derivatives of the von Mises stress at a point with respect to global coordinates x_1 and x_2 are needed to compute. Then the principal quantities in the principal directions X_1 and X_2 where the cross derivatives vanish are determined,

$$\begin{bmatrix} \frac{\partial^2\sigma}{\partial x_1^2} & \frac{\partial^2\sigma}{\partial x_1 \partial x_2} \\ \frac{\partial^2\sigma}{\partial x_1 \partial x_2} & \frac{\partial^2\sigma}{\partial x_2^2} \end{bmatrix} \Rightarrow \begin{bmatrix} \frac{\partial^2\sigma}{\partial X_1^2} & 0 \\ 0 & \frac{\partial^2\sigma}{\partial X_2^2} \end{bmatrix} \tag{11}$$

The maximum principal quantities are then used to compute the proper element size, h_i, by requiring that the error should be uniform for all elements,

$$h_i^2 \lambda_i = h_{min}^2 \lambda_{max} = \text{constant} \tag{12}$$

where $$\lambda_i = \max\left(\left| \frac{\partial^2\sigma}{\partial X_1^2} \right|, \left| \frac{\partial^2\sigma}{\partial X_2^2} \right| \right)$$

λ_{max} is the maximum principal quantity for all elements and h_{min} is the minimum element size specified by users.

6.2 Mesh regeneration

The mesh regeneration with adaptive remeshing technique is implemented based on the Delaunay triangulation and mesh refinement [5]. The main idea is to construct a new mesh over the background mesh (mesh from the previous step). Therefore, the new mesh consists of small elements in the regions with large change in solution gradients and large elements in the other regions where the change in solution gradients in small. The capability of such adaptive remeshing technique will be demonstrated by benchmark examples.

7. Algorithm evaluation

Several examples have been used to demonstrate the efficiency of the combined domain integral, the finite element method, and the adaptive remeshing technique. The examples of a single edge cracked plate, a compact tension specimen and a center cracked plate are used to determine the stress intensity factor in the opening mode under the plane strain condition.

7.1 The single edge cracked plate

The geometry of the single edge cracked plate and its final adaptive mesh are shown in Fig. 4. The stress intensity factor can be calculated from [6],

$$K_I = F\sigma\sqrt{\pi a} \tag{13}$$

where $F = 1.12 - 0.23\alpha + 10.55\alpha^2 - 21.72\alpha^3 + 30.39\alpha^4$

and $\alpha = a/b$

The final adaptive mesh consists of 444 triangles and 931 nodes. The computed stress intensity factor from this adaptive mesh is 2.366 comparing to 2.363 from Eq. (13) with the difference of 0.127%

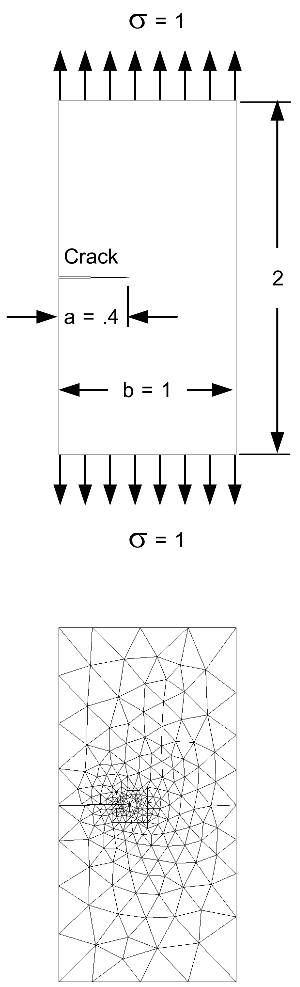

Fig. 4. Problem statement and the final mesh of the single edge cracked plate.

7.2 The compact tension specimen

The geometry of the compact tension specimen and its final adaptive mesh are shown in Fig. 5. The final adaptive mesh consists of 1,396 triangles and 2,939 nodes. The stress intensity factor can be calculated from [7],

$$K_I = P\left(2 + a/w\right)\left[0.886 + 4.64\left(a/b\right) - 13.32\left(a/b\right)^2 + 14.72\left(a/b\right)^3 - 5.6\left(a/b\right)^4\right] / t\sqrt{w}\left(1 - a/w\right)^{3/2} \quad (14)$$

where the thickness $t = 25.4$ mm. The computed stress intensity factor from the adaptive mesh is 28.599 comparing to 27.804 from Eq. (14) with the difference of 2.859%

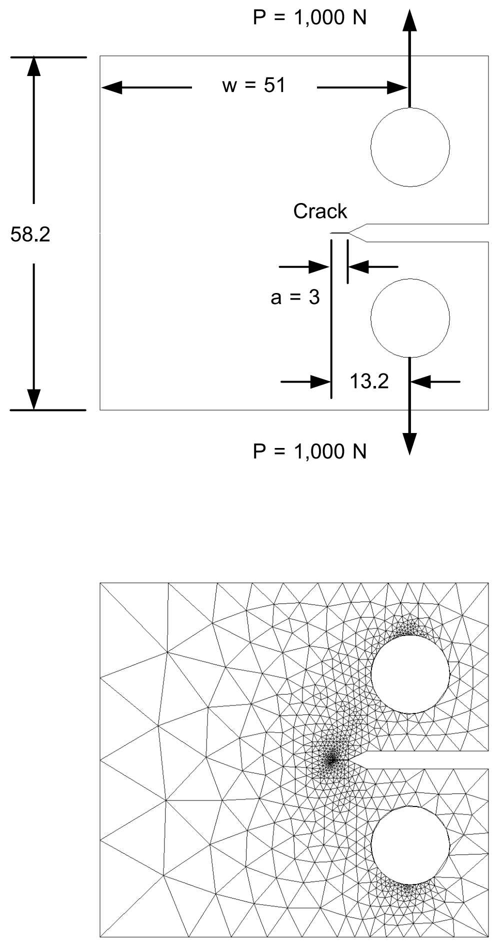

Fig. 5. Problem statement and the final mesh of the compact tension specimen.

7.3 The center cracked plate

The geometry of the center cracked plate and its final adaptive mesh are shown in Fig. 6. The plate has an initial crack length $2a = 100$ units, and the thickness $t = 1$ unit. The stress intensity factor for this problem was derived [8] in closed-form as,

$$K_I = 1.334\sigma\sqrt{\pi a} \quad (15)$$

The final adaptive mesh consists of 1,254 triangles and 2,580 nodes. The computed stress intensity factor from this adaptive mesh is 16.7133 comparing to 16.7192 from Eq. (15) with the difference of 0.04%

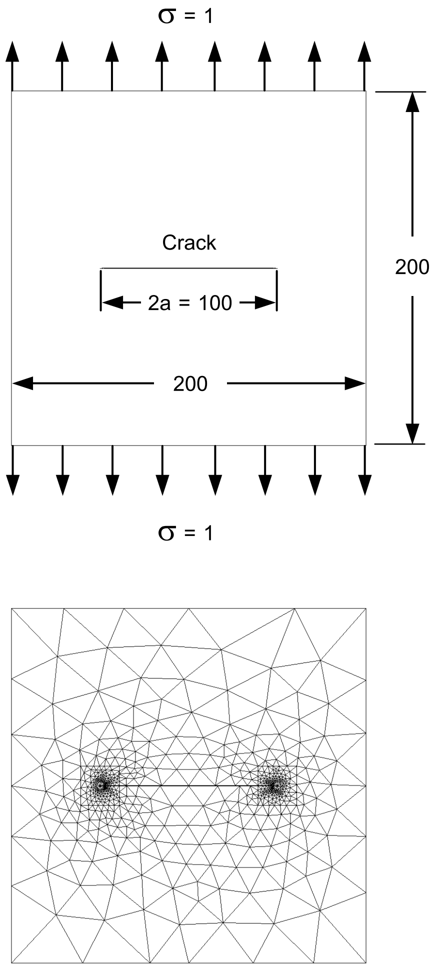

Fig. 6. Problem statement and the final mesh of the center cracked plate.

7.4 Conclusions

Domain integral was combined with the finite element method and the adaptive remeshing technique for analysis of linear elastic fracture mechanics problems. The concept of the domain integral and its smooth function for two-dimensional geometry were explained. The finite element method using the six-node triangular elements was described. These triangular elements with mid-side nodes displaced from their nominal position to a quarter point of the crack tip were employed to form up a circular zone surrounding the crack tip for providing accurate solution. The solution accuracy was further enhanced by incorporating an adaptive remeshing technique. The technique places small elements around the crack tips and in the regions with large change of stress gradients for solution accuracy. At the same, larger elements are generated in the other regions to minimize the total number of unknowns and the computational time.

The efficiency of the combined procedure was demonstrated by examples for determining the stress intensity factor. These examples demonstrate the capability of the combined adaptive remeshing technique with domain integral method for analysis of fracture mechanics problems effectively.

References

[1] T.L. Anderson “Fracture mechanics: fundamentals and applications”, CRC Press, 1995.

[2] C.F. Shih, B. Moran and T. Nakamura “ Energy Release Rate along a Three-dimensional Crack Front in a Thermally Stressed Body”, International Journal of Fracture, 1986, Vol. 30, pp. 79-102.

[3] Y. Omori, A. S. Kobayashi, H. Okada, S. N. Atluri, P. W. Tan “ T_{ε}^{*} integral as a crack growth criterion”, Mechanics of Materials, 1998, Vol. 28, pp. 147-154.

[4] R.S. Barsoum “On the Use of Isoparametric Finite Elements in Linear Fracture Mechanics”, International Journal for Numerical Methods in Engineering, 1976, Vol. 10, pp. 25-37.

[5] P. Dechaumphai, S. Phongthanapanich and P. Bhandhubanyong “Adaptive Delaunay Meshing Technique for Fracture Mechanics Problems”, Key Engineering Materials, 2003, Vol. 233-236, pp. 157-162.

[6] Murakami Y. (Editor) Stress intensity Factors Handbook, Pergamon Press, Oxford, 1987.

[7] ASTM 1996 Annual Book of ASTM Standards, American Society for Testing and Materials, Philadelphia, 1996.

[8] M. Isida ”Effect of Width and Length on Stress Intensity Factors of Internally Cracked Plates Under Various Boundary Conditions”, International Journal of Fracture, 1971, Vol. 7, pp. 301-316.